Nonlinear dynamics of the rattleback: a nonholonomic model

A V Borisov, A O Kazakov, S P Kuznetsov

Contents

Abstract. For a solid convex body moving on a rough horizontal plane — known in mechanics as a rattleback — numerical simulations are used to discuss and illustrate dynamical phenomena that are characteristic of the motion due to the nonholonomic nature of the mechanical system; the relevant feature is the nonconservation of the phase volume in the course of the dynamics evolution. In such a system, a local compression of the phase volume can produce behavior features similar to those exhibited by dissipative systems, such as the presence of stable equilibrium points relevant to stationary rotations; limit cycles (rotations with oscillations), and strange chaotic attractors. A chart of dynamical regimes is plotted in a plane of parameters whose axes are the total mechanical energy and the angle of relative rotation of the geometric and dynamic principal axes of the body. The transition to chaos through a sequence of Feigenbaum period doubling bifurcations is demonstrated. A number of strange attractors are considered, for which phase portraits, Lyapunov exponents, and Fourier spectra are presented.

1. Introduction

Phenomena of complex dynamics, such as chaos and bifurcations, are actively explored in systems of diverse natures, including mechanical ones [1–4].

A V Borisov Udmurt State University,
ul. Universitetskaya 1, 426034 Izhevsk, Russian Federation;
Moscow Institute of Physics and Technology,
Institutskii per. 9, 141700 Dolgoprudnyi, Moscow region,
Russian Federation;
National Research Nuclear University 'MEPhI',
Kashirskoe shosse 31, 115409 Moscow, Russian Federation;
Kalashnikov Izhevsk State Technical University,
ul. Studencheskaya 7, 426069 Izhevsk, Russian Federation
E-mail: borisov@rcd.ru
A O Kazakov Lobachevsky Nizhny Novgorod State University,
prosp. Gagarina 23, 603950 Nizhny Novgorod, Russian Federation
E-mail: kazakovdz@yandex.ru
S P Kuznetsov Saratov Branch of Kotelnikov Institute of
Radioengineering and Electronics, Russian Academy of Sciences,
ul. Zelenaya 38, 410019 Saratov, Russian Federation
E-mail: spkuz@yandex.ru

The definition of a dynamical system assumes that the state given by coordinates in phase space can be obtained from the initial state at an arbitrary instant of time according to some rule that is relevant to this system. Being the ideal case of deterministic description, this definition does not exclude the possibility of chaotic behavior when the state evolution resembles a random process. The main attribute of chaos consists in the sensitivity of motion to small perturbations in initial conditions, which renders impossible predicting the states past some time interval which usually depends logarithmically on errors in initial conditions.

If one considers an ensemble composed of a large number of identical noninteracting systems differing in initial conditions, it corresponds to a cloud of representative points in phase space, which evolves with time varying in size and shape, as dictated by the motion of points according to the dynamical equations of the system.

Traditionally, one distinguishes between *conservative* and *dissipative* dynamical systems.

In physics, the term 'conservative systems' implies systems maintaining energy conservation, which, in particular, relates to systems of classical mechanics described through the Hamilton formalism [5, 6]. Hamiltonian systems obey the Louiville theorem stating the conservation of measure, i.e., the phase volume of each element of the cloud of representative points in the process of dynamics evolution.

In the presence of friction, we have to deal with dissipative systems in which mechanical energy is not conserved but is gradually dissipated by transforming into heat, i.e., the energy of microscopic motion of molecules in the system proper and its surroundings. The phase volume in dissipative systems decreases with time, at least in the mean, and as a result the cloud of representative points 'condenses' at a certain subset in phase space called the *attractor*.[1] For systems wherein the energy loss is compensated for by external sources (open systems), attractors can also be represented, together with equilibrium states (fixed points), by limit cycles, which correspond to self-excited oscillations,

---

[1] It may occur that more than one attractor coexist in phase space; each of the attractors is characterized by its own attraction basin — the set of initial states from which the emitted trajectories arrive at the attractor. In that case, the system is said to be characterized by multistability.

and strange attractors, which correspond to chaotic dynamics.

In systems with invariant measure, i.e., when the Liouville theorem is obeyed (attractors cannot form under these conditions), the cloud of representative points can be regarded as consisting of incompressible fluid, while in the dissipative case it can be considered as a compressible substance (similar to vapor) which may condense, substantially reducing its volume when it precipitates on the attractor.

In mechanics, in addition to systems described in the framework of the Hamilton formalism, one distinguishes a special class of *systems with nonholonomic constraints*, or briefly, *nonholonomic systems* (the term was coined by Heinrich Hertz in the 19th century) [7, 8]. Nonholonomic systems are encountered in many phenomena of large practical significance, for example, in the mechanics of moving or flying apparatuses and in robotics. The history of exploring these systems is rich in dramatic events, including errors made by renowned researchers and then corrected in the course of a more accurate analysis. The hierarchy of the behavioristic types of nonholonomic systems [9, 10] includes various kinds, from simple (integrable) to complex (nonintegrable), which is related to the number of invariants and symmetries intrinsic in the problem under consideration.

We turn now to the problem of the motion of a rattleback — a rigid body with a smooth convex surface — on a rough plane, postulating that the velocity at a contact point between the body and the plane equals zero at any instant of time. Although friction is present in this case, it cannot perform work or, accordingly, change the mechanical energy. Further, let the principal central moments of inertia differ from each other and the geometrical symmetry axes not coincide with the inertia axes. This is the so-called rattleback problem for which the intriguing phenomenon of spin reversal has long been observed [11–13]: after being spun like a top, its rotation is slowed down, accompanied by oscillations (wobbling), and then it starts spinning in the opposite direction.

From a mathematical viewpoint, the fundamental property of the rattleback and nonholonomic systems analogous to it lies in the fact that they lack the invariant measure understood in the sense of the Liouville theorem [14]. This is the principal distinction between objects of nonholonomic mechanics and those of Hamiltonian systems. Although the system is conservative in the sense of conserving mechanical energy and is invariant with respect to the time reversal, the elements of phase space are not conserved in the course of dynamical evolution, undergoing local contraction in some domains in phase space and expansion in others.

The mechanical motion of the rattleback is associated with the displacement of a representative point on a hypersurface of constant energy, with the energy considering as one of the parameters defining the motion character. Owing to phase volume contraction, behavioristic types resembling those of attractors in dissipative systems may occur, for example, stable equilibrium points corresponding to stationary rotation, limit cycles corresponding to rotation with oscillations, and strange attractors [8, 15–17]. Each such object always possesses a symmetric counterpart in phase space, which would become an attracting set when following the dynamics in reversed time. Additionally, dynamical regimes, including chaotic ones, with symmetry to time reversal are possible; they are referred to as 'mixed dynamics' [18].

Thus, we are dealing in this case with a rather specific class of systems falling between the conservative and dissipative systems in the traditional treatment. The goal of this paper is to attract the attention of researches to the problem of dynamics in systems of that kind and illustrate the phenomena of complex dynamics, characteristic for the rattleback, with the results of numerical simulations by resorting to the methods developed previously in studying dissipative systems.

Unusual, sometimes counterintuitive phenomena of the dynamics of rattlebacks could also appear interesting in a conceptual sense for physical problems projecting outside the rigid-body mechanics proper, for example, for the tasks of statistical mechanics of media composed of particles lacking mirror symmetry in geometrical and dynamical characteristics. In this connection, one can mention Ref. [19] treating the dynamical properties of a granulated medium composed of such particles.

2. Rattleback model

Let us turn to a frequently applied model of the rattleback in the shape of an elliptic paraboloid (Fig. 1). Imposing the condition of zero velocity at the contact point, namely

$$\mathbf{v} + \boldsymbol{\omega} \times \mathbf{r} = 0, \tag{1}$$

one may arrive at the following equations for the kinetic momentum $\mathbf{M}$ with respect to the contact point and the unit vector $\boldsymbol{\gamma}$ in the coordinate system linked to the body [8, 16, 17, 20]:

$$\dot{\mathbf{M}} = \mathbf{M} \times \boldsymbol{\omega} + m\dot{\mathbf{r}} \times (\boldsymbol{\omega} \times \mathbf{r}) + mg_0\mathbf{r} \times \boldsymbol{\gamma}, \qquad \dot{\boldsymbol{\gamma}} = \boldsymbol{\gamma} \times \boldsymbol{\omega}. \tag{2}$$

In this case, the vector $\boldsymbol{\omega}$ is linked to the vector $\mathbf{M}$ by the relationship $\mathbf{M} = \mathbf{I}\boldsymbol{\omega} + m\mathbf{r} \times (\boldsymbol{\omega} \times \mathbf{r})$, where $\mathbf{I}$ is the inertia tensor, and the vectors $\boldsymbol{\gamma}$ and $\mathbf{r}$ are coupled by the relationship

$$\boldsymbol{\gamma} = -\frac{\nabla F(r)}{|\nabla F(r)|}, \tag{3}$$
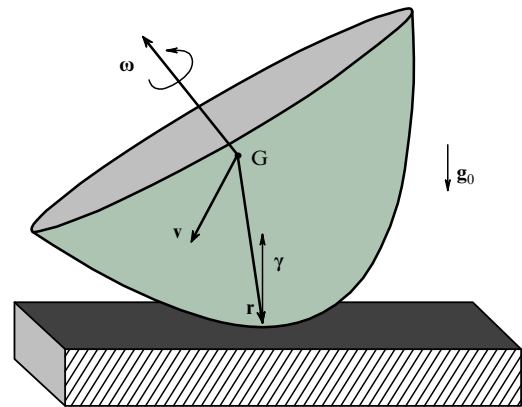

Figure 1. A model of a rattleback: G is the center of mass, $\boldsymbol{\gamma}$ is the unit vector normal to the surface, $\mathbf{r}$ is the vector connecting the center of mass and the contact point, $\mathbf{v}$ is the vector of the velocity of the center of mass, and $\boldsymbol{\omega}$ is the angular velocity vector.

where $F(\mathbf{r}) = 0$ is the equation describing the surface of the body. For an elliptical paraboloid, one obtains

$$F(r) = \frac{1}{2}\left(\frac{r_1^2}{a_1} + \frac{r_2^2}{a_2}\right) - (r_3 + h) = 0,$$

$$r_1 = -\frac{a_1\gamma_1}{\gamma_3}, \quad r_2 = -\frac{a_2\gamma_2}{\gamma_3}, \quad r_3 = -h + \frac{1}{2}\frac{a_1\gamma_1^2 + a_2\gamma_2^2}{\gamma_3^2}. \quad (4)$$

Here, a_1 and a_2 are the principal radii of curvature at the paraboloid vertex, and h is the height of the center of mass located on the paraboloid axis.

We assume that the third principal axis of inertia coincides with the principal geometrical axis $\mathbf{e}_3$, whilst the other two axes of inertia are turned through the angle δ about the geometrical axes. In that case, the tensor of inertia in geometrical axes has the form

$$\mathbf{I} = \begin{pmatrix} I_1\cos^2\delta + I_2\sin^2\delta & (I_1 - I_2)\cos\delta\sin\delta & 0 \\ (I_1 - I_2)\cos\delta\sin\delta & I_1\sin^2\delta + I_2\cos^2\delta & 0 \\ 0 & 0 & I_3 \end{pmatrix}. \quad (5)$$

The constants I_1, I_2, and I_3 are the principal central moments of inertia of the rigid body.

Relationships (2) represent a closed system of equations of the sixth order with respect to vectors γ and $\mathbf{M}$; in order to determine the coordinates of the center of mass (X, Y), one needs to solve, along with Eqns (2), additional equations following from equation (1):

$$\dot{X} = \omega_2 r_3 - \omega_3 r_2, \qquad \dot{Y} = \omega_1 r_3 - \omega_3 r_1. \quad (6)$$

In the course of numerical integration of the system of differential equations (2), a set of three linear algebraic equations relative to the components of the angular velocity vector is solved to compute the right-hand sides at each step of the difference scheme, and additional quantities (4) are computed.

System of equations (2) is characterized by the presence of the geometrical integral $\gamma^2 = 1$, and the energy integral $(1/2)\mathbf{M}\omega - mg_0\mathbf{r}\gamma = E$. In the six-dimensional phase space on the manifold defined by the condition that two integrals of motion be constant, Eqns (2) describe a four-dimensional flow.

We may cut the phase space through by a certain intersecting hypersurface S and take advantage of a Poincaré map. Namely, for any point on the selected hypersurface, the result of the Poincaré mapping will be the point of the next hypersurface intersection by the trajectory leaving the former point. In computations discussed below, the hypersurface was specified by the condition $s = \gamma_1 M_2 - \gamma_2 M_1 = 0$ (taking account that the trajectory passes only in the direction of decreasing s). For a rattleback, the three-dimensional Poincaré map constructed in this manner does not fall in the class of maps preserving phase volume, which allows the existence of stable fixed points, limit circles, and strange attractors.

In the theory of dynamical systems, in order to describe system behavior in the vicinity of some reference phase trajectory, one introduces the Lyapunov exponents [1–4, 21, 22], which characterize exponential, on the average, divergence from (a positive exponent) or convergence to (a negative exponent) the reference trajectory. The total number of exponents equals the phase space dimension, so it is six for system (2), with three of them taking zero values. One zero exponent is associated with infinitesimal perturbation along the reference trajectory, i.e., the perturbation having a type of time shift, and the other two with perturbations of the type relevant to shifts in energy and in the norm of vector γ. One is left with three nontrivial exponents. If we determine the Lyapunov exponents from the Poincaré map, one of the zero exponents immediately drops out of consideration. The other two zero exponents can be excluded if at each step of computing the Poincaré map the vector γ is normalized to unity, and the vector of momentum $\mathbf{M}$ is normalized to a quantity which ensures the given value of the total mechanical energy [17].

3. Phenomena of regular dynamics: reversal and periodic motion

We begin with a model of the rattleback with the parameters utilized in Ref. [16]. Let the principal radii of curvature of the paraboloid be $a_1 = 9$ and $a_2 = 4$, the distance from the vertex to the center of mass $h = 1$, the acceleration due to gravity $g_0 = 100$, the values of the moment of inertia with respect to the main axes $I_1 = 5$, $I_2 = 6$, and $I_3 = 7$, and the angle $\delta = 0.2$. It is known that for this case [2] there is a critical value of the angular velocity of rotation around the vertical axis, $\omega_* = 18.526$, which corresponds to the energy $E_* = 1300$.

If the angular velocity is higher than ω_*, two regimes of rotation in the opposite sense around the vertical axis (vertical spin regimes) exist: stable and unstable. If the rotation is executed in the 'inappropriate' direction, small perturbations of the initial state launch a complex transition process in which oscillations around other coordinate axes emerge. These oscillations, in turn, transform the motion so that a reversal takes place — the sign of angular velocity component ω_3 changes to the opposite one. Figure 2a shows the time evolution of the vertical component of the angular velocity vector which changes its sign as a result of a rather long transition process. Figure 2b depicts the trace left by the contact point on the plane in the course of this process.

As shown in the work by Karapetyan [15], for an angular velocity close to the critical value ω_*, the conditions of the Andronov–Hopf theorem on the birth of the limit cycle become satisfied if the stability loss of the rotation is observed. Passing the threshold ω_* gives birth to a stable limit cycle in place of stable vertical rotation, implying a certain periodic oscillatory solution to the system of equations (2). Figure 3 displays the results of numerical simulations for the regime of motion that corresponds to the Karapetyan cycle: the plots of the time dependence of the kinetic momentum components, the attractor phase portrait in the two-dimensional projection, and the diagram illustrating the motion of the contact point on the plane. Although the velocity and inclination of the rattleback vary strictly periodically with time in the Karapetyan cycle, the trajectory of the contact point remains, in general, open and fills a ring stripe of finite width. Indeed, there are generally no grounds to expect that the ratio of the period of rattleback oscillations to the period it takes the contact point to pass its own trajectory will be expressed by a rational number, so that the motion as a whole proves to be quasiperiodic instead of periodic.

---

[2] The parameters given and the equations written out here correspond to the length measured in centimeters and time in units of $10^{-1/2}$ s for a body 1 kg in mass.
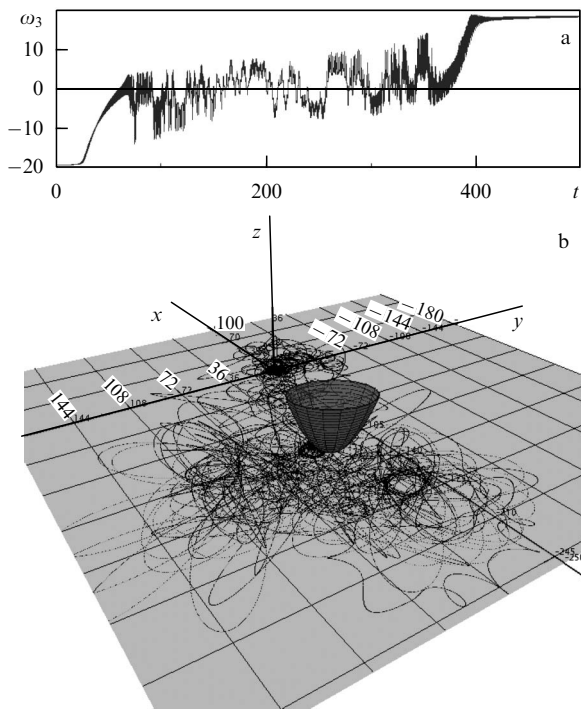
Figure 2. Time dependence of the component ω_3 of angular velocity illustrating the reversal effect (a), and the trace left on the plane by the contact point in the course of this process (b) for $E = 1380$, $I_1 = 5$, $I_2 = 6$, $I_3 = 7$, $g_0 = 100$, $a_1 = 9$, $a_2 = 4$, $h = 1$, and $\delta = 0.2$.

4. Phenomena of complex dynamics

Turning to the consideration of complex dynamics, we set for a rattleback shaped like an elliptic paraboloid the principle moments of inertia at $I_1 = 2$, $I_2 = 6$, and $I_3 = 7$, taking, as earlier, $a_1 = 9$, $a_2 = 4$, $h = 1$, and $g_0 = 100$ [17]. In this case, stable vertical rotation is absent, even for large energies, and the general pattern of dynamical behavior as a function of the parameters E (energy) and δ (the angle of rotation of the inertia axes relative to the geometrical axes) proves to be amazingly rich.

Figure 4 demonstrates the regime diagram for the Poincaré mapping of the system under consideration on the parameter plane $(E - \delta)$. To construct the diagram, an exhaustion of mesh nodes in the plane (E, δ) with some mesh width over both parameters has been carried out. At each mesh point, about 10^3 iterations of the Poincaré map have been performed, and the results of the last iterations have been analyzed with regard to the presence of the repetition period within some given level of admissible errors. On discovering the periodicity, the respective pixel in the diagram was marked in a designated color, and the analysis shifted to the next point in the parameter plane. In so doing, it was reasonable to start iterations at a new point from the state obtained as a result of iterations at the preceding point ('scanning with inheritance'), which in most cases warrants acceleration of convergence to the steady regime of dynamics. In constructing the diagram presented in Fig. 4, the results of scanning with inheritance in directions from left to right and from bottom to top have been used. The color coding rule is provided in the right part of the figure, and the period was determined by following the dynamics of the angular momentum component M_3.
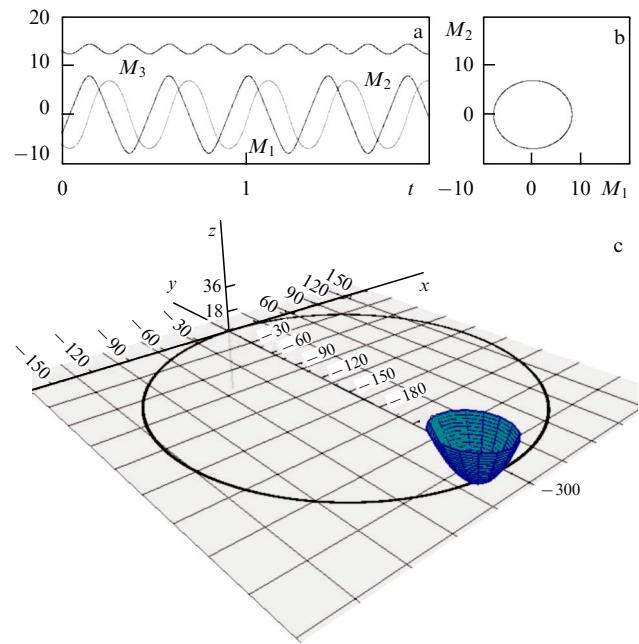

Figure 3. Time dependence of the angular momentum components (a); the phase portrait of the attractor in the projection onto the plane $M_1 - M_2$ (b), and the trajectory of motion of the point of contact between the body and the plane (c) in the Karapetyan cycle for $E = 1000$, $I_1 = 5$, $I_2 = 6$, $I_3 = 7$, $g_0 = 100$, $a_1 = 9$, $a_2 = 4$, $h = 1$, and $\delta = 0.2$.
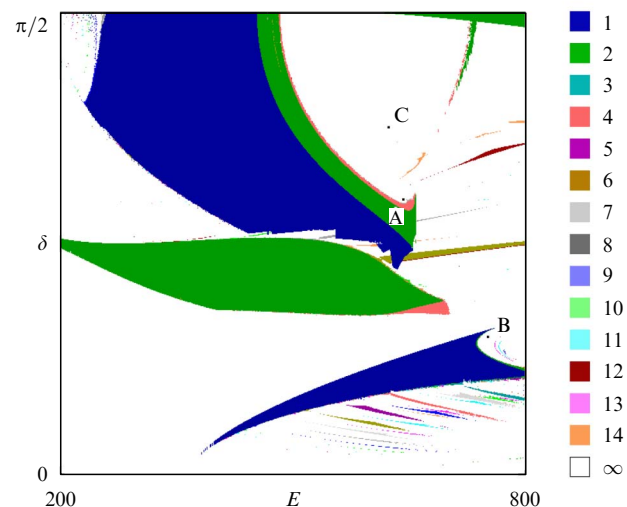

Figure 4. (Color online.) Diagrams of the regimes of motion on the parameter plane of the energy E – angle δ of rotation of the inertia axes with respect to the geometrical axes for the Poincaré map of a rattleback shaped as an elliptic paraboloid at $I_1 = 2$, $I_2 = 6$, $I_3 = 7$, $g_0 = 100$, $a_1 = 9$, $a_2 = 4$, and $h = 1$.

We will consider in more detail the attractors which are realized at points A, B, and C in the diagram of Fig. 4.

If one moves upward in the parameter plane along the vertical line passing through point A, a transition to chaos via the sequence of bifurcations of period doubling can be observed. This is illustrated by the tree-like diagram in Fig. 5a, which displays a characteristic pattern of branches, pinching off at bifurcation points, and the 'crown' filled with points that corresponds to the chaos region. Figure 5b zooms in on parts of the pattern, which, upon magnification, more
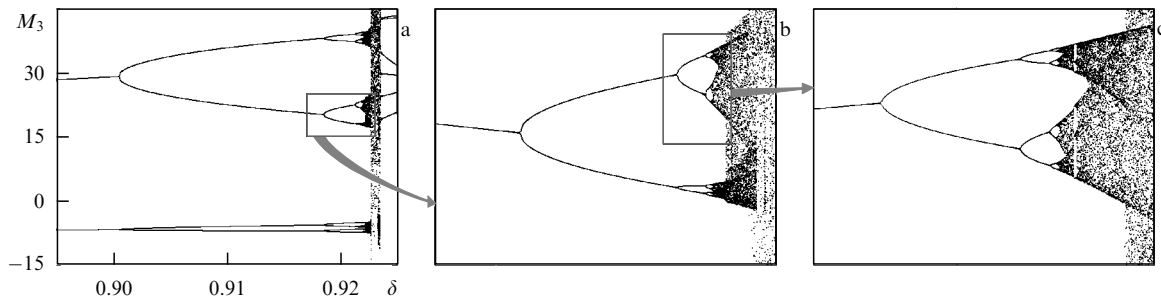
Figure 5. Bifurcation trees in the domain of transition to chaos through period doublings according to Feigenbaum for the parameters $I_1 = 2$, $I_2 = 6$, $I_3 = 7$, $g_0 = 100$, $a_1 = 9$, $a_2 = 4$, $h = 1$, and $E = 642$. Scanning is carried out toward the larger parameter δ, with inherited initial conditions.

Table 1. Estimates of the Feigenbaum constants.

	(2.4)/(4.8)	(4.8)/(8.16)	(8.16)/(16.32)	(32.64)/(64.128)	Feigenbaum constants
δ_F	6.52	5.29	4.70	4.62	4.6692
α_F	−3.79	−2.82	−2.64	−2.54	−2.5029

and more resemble the classical pattern of the 'Feigenbaum tree' for one-dimensional maps [21, 22].

Measuring the horizontal intervals between branch splitting in the diagram and computing their ratios for subsequent doubling levels, we obtain the first row of Table 1. Likewise, having determined the ratios of intervals between branch splitting in the vertical direction, we fill in the second row. For the transition to be in the Feigenbaum universality class [21–24], the ratios must converge to the universal constants $\delta_F \approx 4.6692$ and $\alpha_F \approx -2.5029$. It can be seen from Table 1 that this is the case. The fact that the estimates of constants are larger in absolute value at the first levels of doubling is linked to the *crossover effect* [25]. Given the small effective dissipation (understood as the characteristics of 3D phase volume contraction in the given domain in phase space), the constants at low levels are close to those characteristic of doubling in conservative systems: $\delta_H \approx 8.721$ and $\alpha_H \approx -4.018$ [26, 27]. Upon each subsequent bifurcation, the degree of contraction is doubled over the characteristic period, and the estimates tend asymptotically to the universal constants δ_F and α_F.

The attractor of the three-dimensional Poincaré map, emerging as the result of the cascade of period doubling, is shown in Fig. 6 for point A ($E = 642$, $\delta = 0.922$) in the projection onto the plane of variables M_1 and M_2. Visually, it resembles attractors of dissipative maps observed immediately beyond the threshold of transition to chaos through period doublings. The figure also shows the spectrum of oscillations of variable M_3 for the dynamics on the attractor. The spectrum contains a set of peaks with a hierarchic structure characteristic of an attractor appearing through the Feigenbaum cascade [21, 22, 24]. According to Feigenbaum, the peaks of each subsequent level should be, on average, 13.4 dB lower than at the preceding level, which agrees well with the observed picture. The peaks at deep levels are broken, giving way to a continuous spectrum, i.e., the dynamics become chaotic.

The Lorenz attractor [28, 29] constitutes the already classical object of nonlinear dynamics and chaos theory, which falls in the class of singular-hyperbolic, or quasihyperbolic, attractors. For many years, the Lorenz model was a subject of active and rigorous research [29–31]. Its summary
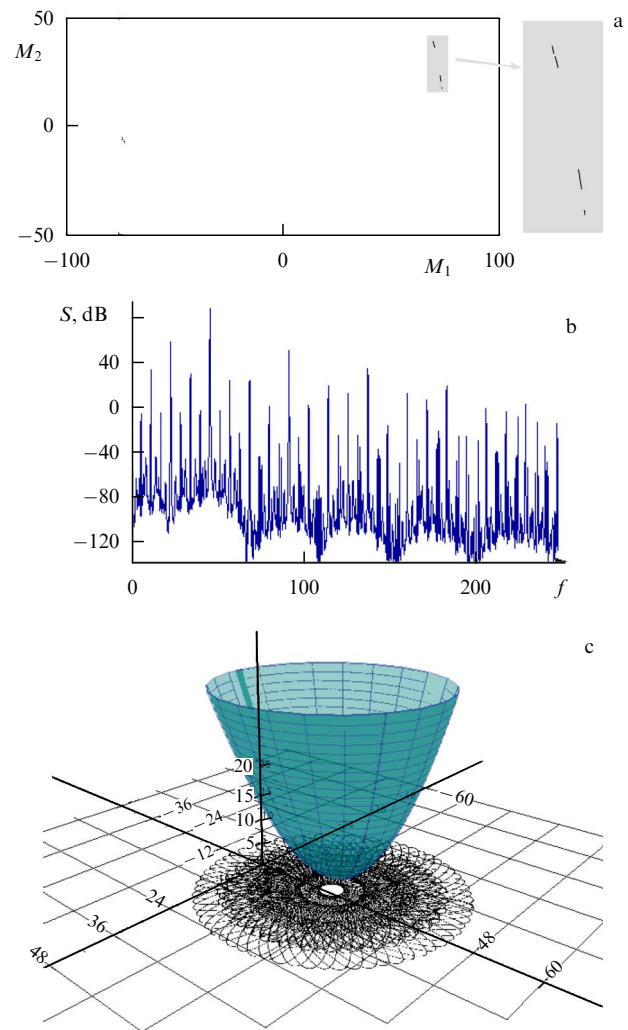

Figure 6. The portrait of an attractor in the Poincaré section in a projection onto the plane of two components of angular momentum (a), the Fourier spectrum for the component M_3 (b), and the trace left on the plane by the contact point (c) for the dynamics on the attractor. The parameters are as follows: $I_1 = 2$, $I_2 = 6$, $I_3 = 7$, $g_0 = 100$, $a_1 = 9$, $a_2 = 4$, $h = 1$, $E = 642$, and $\delta = 0.922$.
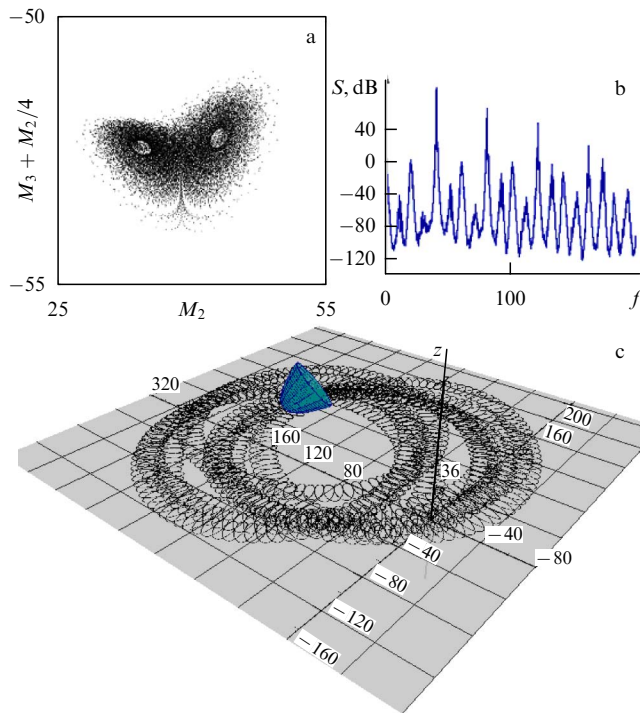
Figure 7. Portrait of an attractor in the Poincaré section in a projection onto the plane of two angular momentum components (a), the Fourier spectrum of the component M_3 (b), and the trace left by the contact point (c) on the plane for the dynamics on the attractor. The problem parameters are as follows: $I_1 = 2$, $I_2 = 6$, $I_3 = 7$, $g_0 = 100$, $a_1 = 9$, $a_2 = 4$, $h = 1$, $E = 752$, and $\delta = 0.485$.

Figure 8. Portrait of an attractor in the Poincaré section in a projection onto the plane of two angular momentum components (a), the Fourier spectrum of the component M_3 (b), and the trace left by the contact point (c) on the plane for the dynamics on the attractor. The parameters are as follows: $I_1 = 2$, $I_2 = 6$, $I_3 = 7$, $g_0 = 100$, $a_1 = 9$, $a_2 = 4$, $h = 1$, $E = 620$, and $\delta = 1.178$.

result was accurate mathematical substantiation of the chaotic nature of the dynamics on the Lorenz attractor, which was given relatively recently by W Tucker [32] based on a combination of computer-assisted proof and accurate analytical consideration. In this respect, the discovery of quite a general situation in which a Lorenz type attractor is born as a result of a certain sequence of bifurcation events in three-dimensional maps seems interesting and remarkable [18]. This attractor arises when, after the bifurcation of period doubling, the newly appeared double-periodic orbit loses its stability because of the Neimark–Sacker bifurcation (and not as a result of secondary doubling), upon which the unstable manifold of the primary periodic point having lost its stability intersects the stable two-dimensional manifold of the point. As it turned out, this is also related, in particular, to the three-dimensional Poincaré map for the nonholonomic model of rattlebacks [33].

An example of a Lorenz type attractor in the Poincaré map for a rattleback is given in Fig. 7 in a two-dimensional projection, together with the spectrum of oscillations of the variable M_3, and a diagram illustrating the motion of the contact point along the plane. The problem parameters, selected as described in Ref. [33], correspond to point B in Fig. 4.

As is easy to ascertain, the representative point performs jumps in iterations of the Poincaré map, visiting, in an alternating manner, the 'curls' of the attractor—left and right ones. For the map conforming to a two-fold iteration, subsequent positions of the representative point can be conceived of as belonging to a continuous trajectory of some approximating flow system with a Lorenz attractor.
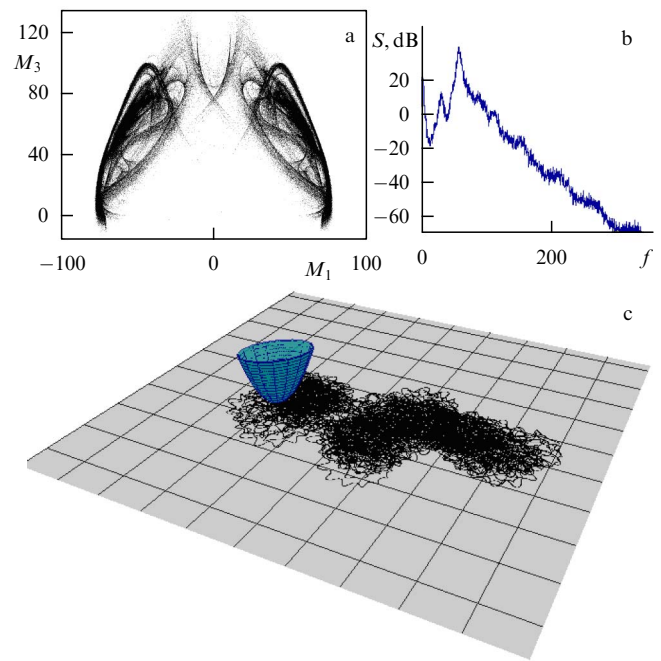
For this attractor, the Lyapunov exponents of the three-dimensional map are, according to computations, $\Lambda_1 = 0.0202$, $\Lambda_2 = 0.0000$, and $\Lambda_3 = -0.1925$. The first one is positive, which points to the existence of chaos. This can also be judged by the character of the spectrum in Fig. 7b which, as can be seen, is continuous, albeit rather irregular. The second exponent is close to zero, which is linked to the possibility of describing the dynamics with the help of the approximating flow system. The third one is negative, making the sum of all exponents negative too, which ensures the contraction of the phase volume to zero in the dynamic process which ends at the attractor. The dimension of the attractor in the Poincaré map estimated by the Kaplan–Yorke formula [21, 22] is $D = 2 + (\Lambda_1 + \Lambda_2)/|\Lambda_3| \approx 2.10$, which slightly exceeds two, the same as for the classical Lorenz attractor.

Figure 8 displays the attractor at point C ($E = 620$, $\delta = 3\pi/8$) and the Fourier spectrum which is apparently related to well-developed chaos. The irregularity of this spectrum, in contrast to the irregularity of the spectra in Figs 6 and 7, is not strong, which attests to the absence of any substantial periodic components of motion. The Lyapunov exponents are here as follows: $\Lambda_1 = 0.282$, $\Lambda_2 = -0.093$, and $\Lambda_3 = -0.686$. The first Lyapunov exponent is positive, while the second one is negative but smaller than the first one in absolute value. For this reason, the dimension according to the Kaplan–Yorke formula exceeds two: $D = 2 + (\Lambda_1 + \Lambda_2)/|\Lambda_3| \approx 2.26$.

5. Conclusions

This article presents materials of the computer-assisted study on the dynamics of the nonholonomic model of a rattle-

back — a dynamical system of a specific type which occupies an intermediate place between conservative and dissipative systems in the common sense. On the one hand, the system considered here possesses mechanical energy conservation and is invariant to time reversal; on the other hand, it does not preserve phase volume, which may locally experience contraction or expansion. For this reason, one may observe on the hypersurface of constant energy in phase space a dynamical behavior of the system which, on a large time scale, is defined by attracting sets — the attractors. They include fixed points associated with stable rotations, limit cycles which correspond to rotations with oscillations, and strange chaotic attractors. From the methodical viewpoint, the presence of attractors makes using techniques applied thus far to dissipative dynamical systems both natural and relevant, which we demonstrated with concrete examples. Apparently, a similar approach can also be productive for other mechanical systems capable of demonstrating phenomena of complex dynamics.

In the theories of oscillations and nonlinear dynamics, it is frequently assumed, either explicitly or implicitly, that attention should only be paid to rough (structurally-stable) phenomena, which implies the insensitivity of dynamical regimes to variations in parameters and characteristics of models and systems, thus ensuring the observability of these phenomena in practice. However, following this rule in a literal way is not always appropriate. For example, Hamiltonian systems, being a subset of all possible dynamical systems, are certainly not rough, because they may be expelled from their class by an infinitesimally small variation of the right-hand sides of their differential equations. The history of science witnesses that this has not led to abandoning studies of Hamiltonian systems, although the question of observability of their intrinsic dynamic phenomena in experiment frequently proves to be anything but trivial.

Thus, under certain conditions, one phenomenon or another may correctly correspond to the dynamics on finite time intervals, but the description may cease to be relevant at large time, for example, because of dissipation, however small as is desired. Similar reservations should be made with respect to the nonholonomic model of a rattleback considered here, at least with respect to its conservativity in the sense of mechanical energy conservation. Indeed, this model assumes a far going idealization in the problem statement since, in a realistic physical system, the nonholonomic constraint can be violated, so that obtaining a theoretical description, rigorous in detail, would demand attention for actual friction laws which violate the conservative nature of the system.

For the rattleback, a useful discussion of the relation of various theoretical models to the actual experiment has been carried out, notably, in Ref. [34]. As a well-known example for which the nonholonomic model clearly fails, one may mention the description of the Thompson top, also known as the 'Chinese top' [35, 36].

Nevertheless, the nonholonomic model proves to be useful and insightful, allowing one to explain numerous phenomena observed with real rattlebacks, including reversal, multiple reversals, Karapetyan cycles, and chaotic oscillations over finite time intervals. From the viewpoint of quantitative correspondence to actual experiments, the results obtained in the framework of the nonholonomic model should be taken with caution (including those related to the trajectory of the contact point).

References

1. Lichtenberg A J, Lieberman M A *Regular and Stochastic Motion* (New York: Springer-Verlag, 1983); Translated into Russian: *Regulyarnaya i Stokhasticheskaya Dinamika* (Moscow: Mir, 1984)
2. Sagdeev R Z, Usikov D A, Zaslavsky G M *Nonlinear Physics*: *From the Pendulum to Turbulence and Chaos* (Chur: Harwood Acad. Publ., 1988); Translated from Russian: Zaslavsky G M, Sagdeev R Z *Vvedenie v Nelineinuyu Fiziku*: *Ot Mayatnika do Turbulentnosti i Khaosa* (Moscow: Nauka, 1988)
3. Rabinovich M I, Trubetskov D I *Oscillations and Waves in Linear and Nonlinear Systems* (Dordrecht: Kluwer Acad. Publ., 1989); Translated from Russian: *Vvedenie v Teoriyu Kolebanii i Voln* (Moscow: Nauka, 1984)
4. Landa P S *Nelineinye Kolebaniya i Volny* (Nonlinear Oscillations and Waves) (Moscow: Librokom, 2010)
5. Landau L D, Lifshitz E M *Mechanics* (Oxford: Pergamon Press, 1976); Translated from Russian: *Mekhanika* (Moscow: Nauka, 1973)
6. Arnold V I *Mathematical Methods of Classical Mechanics* (New York: Springer, 1997); Translated from Russian: *Matematicheskie Metody Klassicheskoi Mekhaniki* (Moscow: Nauka, 1989)
7. Borisov A V, Mamaev I S (Eds) *Negolonomnye Dinamicheskie Sistemy. Integriruemost', Khaos, Strannye Attraktory* (Nonholonomic Dynamical Systems: Integrability, Chaos, and Strange Attractors) (Moscow–Izhevsk: Inst. Komp. Issled., 2002)
8. Neimark Ju I, Fufaev N A *Dynamics of Nonholonomic Systems* (Providence, R.I.: American Mathematical Society, 1972); Translated from Russian: *Dinamika Negolonomnykh Sistem* (Moscow: Nauka, 1967)
9. Borisov A V, Mamaev I S *Regular Chaotic Dynamics* **7** 177 (2002)
10. Borisov A V, Mamaev I S, Bizyaev I A *Nelin. Din.* **9** 141 (2013)
11. Walker G T *Proc. Cambr. Phil. Soc.* **8** 305 (1895)
12. Walker G T *Quart. J. Pure Appl. Math.* **28** 175 (1896)
13. Walker J *Sci. Am.* **241** (10) 144 (1979)
14. Kozlov V V *Usp. Mekh.* **8** (3) 85 (1985)
15. Karapetyan A V *Izv. Akad. Nauk SSSR Mekh. Tverd. Tela* (2) 19 (1985)
16. Borisov A V, Mamaev I S *Phys. Usp.* **46** 393 (2003); *Usp. Fiz. Nauk* **173** 407 (2003)
17. Borisov A V et al. *Regular Chaotic Dynamics* **17** 512 (2012)
18. Gonchenko A S, Gonchenko S V, Shil'nikov L P *Nelin. Din.* **8** (1) 3 (2012)
19. Tsai J-C et al. *Phys. Rev. Lett.* **94** 214301 (2005)
20. Gonchenko A S, Gonchenko S V, Kazakov A O *Nelin. Din.* **8** 507 (2012)
21. Schuster H G, Just W *Deterministic Chaos*: *An Introduction* (Weinheim: Wiley-VCH, 2005); Translated into Russian: *Determinirovannyi Khaos* (Moscow: Mir, 1988)
22. Kuznetsov S P *Dinamicheskii Khaos* (Dynamical Chaos) (Moscow: Fizmatlit, 2006)
23. Feigenbaum M J *J. Stat. Phys.* **21** 669 (1979)
24. Vul E B, Sinai Ya G, Khanin K M *Russ. Math. Surv.* **39** 1 (1984); *Usp. Mat. Nauk* **39** (3) 3 (1984)
25. Reick C *Phys. Rev. A* **45** 777 (1992)
26. Reichl L E *The Transition to Chaos*: *Conservative Classical Systems and Quantum Manifestations* (New York: Springer, 2004); Translated into Russian: *Perekhod k Khaosu v Konservativnykh Klassicheskikh i Kvantovykh Sistemakh* (Moscow–Izhevsk: RKhD, 2008)
27. Kuznetsov S P, Kuznetsov A P, Sataev I R *J. Stat. Phys.* **121** 697 (2005)
28. Lorenz E N *J. Atmos. Sci.* **20** 130 (1963); Translated into Russian: *Strannye Attraktory* (Eds Ya G Sinai, L P Shil'nikov) (Moscow: Mir, 1981) p. 88

29. Sparrow C *The Lorenz Equations: Bifurcations, Chaos, and Strange Attractors* (New York: Springer-Verlag, 1982)

30. Afraimovich V S, Bykov V V, Shil'nikov L P *Sov. Phys. Dokl.* **22** 253 (1977); *Dokl. Akad. Nauk SSSR* **234** 336 (1977)

31. Guckenheimer J, Holmes P *Nonlinear Oscillations, Dynamical Systems, and Bifurcations of Vector Fields* (Berlin: Springer, 1990); Translated into Russian: *Nelineinye Kolebaniya, Dinamicheskie Sistemy i Bifurkatsii Vektornykh Polei* (Moscow–Izhevsk: Inst. Komp. Issled., 2002)

32. Tucker W *Found. Comput. Math.* **2** 53 (2002)

33. Gonchenko A S, Gonchenko S V *Nelin. Din.* **9** (1) 77 (2013)

34. Garcia A, Hubbard M *Proc. R. Soc. Lond. A* **418** 165 (1988)

35. Kane T R, Levinson D A, in *American Society of Mechanical Engineers, Winter Annual Meeting, San Francisco, Calif., Dec. 10 – 15, 1978*

36. Aleshkevich V A, Dedenko L G, Karavaev V A *Lektsii po Mekhanike Tverdogo Tela* (Lectures on Mechanics of Solids) (Moscow: Izd. MGU, 1997)